

On the Message Passing Efficiency of Polar and Low-Density Parity-Check Decoders

Dawei Yin, Yuan Li, Xianbin Wang, Jiajie Tong, Huazi Zhang,
Jun Wang, Guanghui Wang, Guiying Yan, and Zhiming Ma

Abstract

This study focuses on the efficiency of message-passing-based decoding algorithms for polar and low-density parity-check (LDPC) codes. Both successive cancellation (SC) and belief propagation (BP) decoding algorithms are studied under the message-passing framework. Counter-intuitively, SC decoding demonstrates the highest decoding efficiency, although it was considered a weak decoder regarding error-correction performance. We analyze the complexity-performance tradeoff to dynamically track the decoding efficiency, where the complexity is measured by the number of messages passed (NMP), and the performance is measured by the statistical distance to the maximum *a posteriori* (MAP) estimate. This study offers new insight into the contribution of each message passing in decoding, and compares various decoding algorithms on a message-by-message level. The analysis corroborates recent results on terabits-per-second polar SC decoders, and might shed light on better scheduling strategies.

Index Terms

decoding efficiency, probability codes, belief propagation, successive cancellation.

This work is partially supported by the National Natural Science Foundation of China (11631014) and Shandong University Multidisciplinary Research and Innovation Team of Young Scholars.

Dawei Yin is with the School of Mathematics, Shandong University, Jinan, 250100 China, and also with the Huawei Technologies Co. Ltd., Hangzhou, 310051 China (e-mail: daweiyin@mail.sdu.edu.cn).

Yuan Li is with the Academy of Mathematics and Systems Science, CAS, University of Chinese Academy of Sciences, Beijing, 100190 China, and also with the Huawei Technologies Co. Ltd., Hangzhou, 310051 China (e-mail: liyuan181@mails.ucas.ac.cn).

Xianbin Wang, Jiajie Tong, Huazi Zhang, and Jun Wang are with the Huawei Technologies Co. Ltd., Hangzhou, 310051 China (e-mail: {wangxianbin1, tongjiajie, zhanghuazi, justin.wangjun}@huawei.com).

Guanghui Wang is with the School of Mathematics, Shandong University, Jinan, 250100 China (e-mail: ghwang@sdu.edu.cn).

Guiying Yan and Zhiming Ma are with the Academy of Mathematics and Systems Science, CAS, University of Chinese Academy of Sciences, Beijing, 100190 China (e-mail: yangy@amss.ac.cn; mazm@amt.ac.cn).

I. INTRODUCTION

AFTER over six decades of research efforts, probabilistic coding and polar coding can approach the theoretical Shannon limit under additive white Gaussian noise (AWGN) channel, both in the asymptotic and finite-length regimes [1]–[4]. Shannon’s paradigm focuses on two dimensions: *probability of decoding error* versus *noise level*. The former is measured by bit error rate (BER) or block error rate (BLER), and the latter is measured by signal-to-noise ratio (SNR). The “SNR-BLER” curve and its gap to channel capacity have become the primary criterion for comparing different coding and decoding schemes. This paradigm has guided coding theory and practice toward a tremendous success. In practice, there are other dimensions of interest, such as complexity, latency, and energy efficiency. In the 1960s, E. R. Berlekamp noted that “*from a practical standpoint, the essential limitation of all coding and decoding schemes proposed to date has not been Shannon’s capacity but the complexity of the decoder*” [5]. Although Berlekamp referred to algebraic codes, his observation holds to this day. Complex decoding algorithms can hardly be adopted for implementation even if they approach channel capacity. This is particularly true as Moore’s law has almost reached the physical limits [6].

Recently, terabits-per-second (Tbps) high throughput decoders were reported from both academia and industry [7]–[9]. Polar SC decoders can achieve a record-breaking throughput of 1.5 Tbps [8] and 4 Tbps [9] within only one square millimeter chip area. These results prove the high decoding efficiency of polar SC decoders, although they were considered weak from the error-correction performance perspective [10]–[13]. High-efficiency decoders are instrumental in delivering Tbps peak throughput services for 6G. It prompts us to explore the theoretical analysis of decoding efficiency, in addition to the well-researched decoding performance. In particular, we need to define a metric to analyze decoding efficiency quantitatively.

Decoding efficiency, characterized by a complexity-performance tradeoff, varies across different decoding algorithms. In the research of sequential decoding, the cutoff rate has become an essential index for describing the complexity-performance tradeoff [14]. The average per-bit complexity is a finite constant when obtaining performance below the cutoff rate and grows exponentially if the code rate is above the cutoff rate [15]. J. L. Massey suggested that, as a rule of thumb, the cutoff rate is the practical upper limit on code rates for reliable communications, whereas capacity is the theoretical upper limit [16]. In message-passing decoding, R. J. McEliece conjectures that for a large class of channels, if the designed rate of code ensemble equals a

fraction $1 - \epsilon$ of the channel capacity, then the decoding complexity scales like $\frac{1}{\epsilon} \ln \frac{1}{\epsilon}$ [17]. Still, this conjecture does not enable quantitative comparisons among message-passing algorithms.

This study aims at measuring the decoding efficiency of two well-known codes, that is, polar codes and low-density parity-check (LDPC) codes [18]. Specifically, we focus on successive cancellation (SC) decoding for polar codes and belief propagation (BP) decoding for both codes. In the general sense, both SC and BP are message-passing algorithms on a factor graph. To characterize the complexity-performance tradeoff, we adopt a two-dimensional paradigm, where the complexity is measured by the number of messages passed (NMP), and the performance is measured by a metric based on the Bethe free energy (to be described shortly). The fine-grained definition of NMP allows to measure BP decoding complexity on a message-by-message level, as opposed to a coarse-grained complexity analysis on the iteration level [19]. The NMP can also measure the complexity of SC decoding for polar codes, as SC is BP with special scheduling [20]. Measuring decoding performance by BER/BLER is a common practice. However, it offers little insight into the internal decoding process, thus does not serve our purpose. Alternatively, we propose to look into the convergence of decoding process by tracking “*how far away is an intermediate decoding state from the maximum a posteriori (MAP) decoding result*”, coined as “Gap to maximum A Posteriori (GAP)”. To this end, we derive GAP based on Bethe free energy to measure the statistical distance between the distribution obtained by message passing and the true posterior distribution. It offers two distinctive advantages. First, it zooms in on each individual edge’s log-likelihood ratio (LLR) update in the decoding process, thus providing a higher resolution than traditional extrinsic information transfer (EXIT) chart methods for analyzing iterative decoders. Second, the “NMP-GAP” curve can be efficiently obtained by Monte Carlo simulations or density evolution (DE) [2]. This paradigm allows us to quantitatively study the decoding efficiency of message-passing algorithms and may inspire new approaches for improving efficiency.

The paper is organized as follows: Section II introduces some basic concepts and several decoding algorithms. In Section III, we illustrate the rationality of adopting the “NMP-GAP” curve to study decoding efficiency. In Section IV, we introduce the advantages of the “NMP-GAP” paradigm and apply it to compare the efficiency of several algorithms. In Section V, we apply this model to the scheduling policy of LDPC codes. We conclude in Section VI.

II. PRELIMINARIES

In this section, we review the BP and SC algorithms from the perspective of decoding efficiency.

A. LDPC codes and the BP decoding

A binary LDPC code with a parity check matrix H can be represented by a factor graph $G = (\mathcal{V} \cup \mathcal{C}, \mathcal{E})$ [21], where \mathcal{V} and \mathcal{C} are the disjoint sets of variable nodes (VNs) and check nodes (CNs), respectively, and \mathcal{E} is the set of edges connecting the VNs and CNs.

BP decoding proceeds by successively passing messages on the factor graph between VNs (denoted by i) and CNs (denoted by α). Example of LDPC and polar factor graphs are shown in Fig. 1.

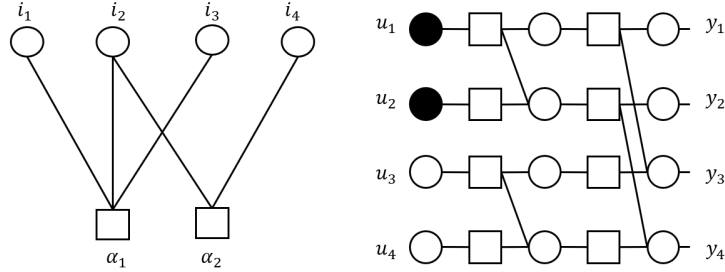


Fig. 1. (4,2) LDPC and Polar codes. Let circles denote variable nodes, boxes denote check nodes, and solid circles be the frozen bits of polar code.

For the sum-product algorithm [22], the update rule for a variable-to-check (V2C) LLR message is

$$m_{i \rightarrow \alpha}^{(l)} = m_0 + \sum_{h \in N(i) \setminus \alpha} m_{h \rightarrow i}^{(l-1)}, \quad (1)$$

and the update rule at a check-to-variable (C2V) edge is

$$m_{\alpha \rightarrow i}^{(l)} = 2 \tanh^{-1} \left(\prod_{j \in N(\alpha) \setminus i} \tanh \left(m_{j \rightarrow \alpha}^{(l-1)} / 2 \right) \right), \quad (2)$$

where m_0 is the channel message in LLR form, l is the number of iterations, $N(v)$ represents the nodes connected directly to node v , $i \rightarrow \alpha$ means from variable node i to check node α and $\alpha \rightarrow i$ means from check node α to variable node i . The initial message $m_{i \rightarrow \alpha}^{(0)}$ and $m_{\alpha \rightarrow i}^{(0)}$ is 0.

The min-sum approximation in [23] can be employed to reduce the complexity of (2):

$$m_{\alpha \rightarrow i}^{(l)} \approx \prod_{j \in N(\alpha) \setminus i} \text{sign} \left(m_{j \rightarrow \alpha}^{(l-1)} \right) \cdot \min_{j \in N(\alpha) \setminus i} \left(\left| m_{j \rightarrow \alpha}^{(l-1)} \right| \right). \quad (3)$$

B. Polar codes and the SC decoding

A polar code can be denoted by (n, k, \mathcal{A}) , where n is the code length and \mathcal{A} is a set of information indices that carry k information bits $\mathbf{u}_{\mathcal{A}}$. The complement of \mathcal{A} is the frozen indices \mathcal{A}^c that carry frozen bits $\mathbf{u}_{\mathcal{A}^c}$. The polar generator matrix is $\mathbf{G}_n = \mathbf{B}_n \mathbf{F}^{\otimes s}$ for any $n = 2^s$, where \mathbf{B}_n is a bit-reversal permutation matrix, $\mathbf{F}^{\otimes s}$ denotes the s -th Kronecker power of $\mathbf{F} \triangleq \begin{bmatrix} 1 & 0 \\ 1 & 1 \end{bmatrix}$. A codeword is generated by $\mathbf{c} = \mathbf{u} \mathbf{G}_n$, where $\mathbf{u} = (\mathbf{u}_{\mathcal{A}}, \mathbf{u}_{\mathcal{A}^c})$.

SC decoder for polar code estimates u_i for given frozen bits $\mathbf{u}_{\mathcal{A}^c}$, received word \mathbf{y} and the estimates $\hat{\mathbf{u}}_1^{i-1}$ of \mathbf{u}_1^{i-1} [1]. It can be implemented by computing LLR $L_n^{(i)}(\mathbf{y}_1^n, \hat{\mathbf{u}}_1^{i-1}) \triangleq \ln \frac{W_n^{(i)}(\mathbf{y}_1^n, \hat{\mathbf{u}}_1^{i-1} | 0)}{W_n^{(i)}(\mathbf{y}_1^n, \hat{\mathbf{u}}_1^{i-1} | 1)}$ ($1 \leq i \leq n$) according to the recursive formula:

$$L_n^{(2j-1)}(\mathbf{y}_1^n, \hat{\mathbf{u}}_1^{2j-2}) = F\left(L_{n/2}^{(j)}\left(\mathbf{y}_1^{n/2}, \hat{\mathbf{u}}_{1,o}^{2j-2} \oplus \hat{\mathbf{u}}_{1,e}^{2j-2}\right), L_{n/2}^{(j)}\left(\mathbf{y}_{n/2+1}^n, \hat{\mathbf{u}}_{1,e}^{2j-2}\right)\right), \quad (4)$$

and

$$L_n^{(2j)}(\mathbf{y}_1^n, \hat{\mathbf{u}}_1^{2j-1}) = G\left(L_{n/2}^{(j)}\left(\mathbf{y}_1^{n/2}, \hat{\mathbf{u}}_{1,o}^{2j-2} \oplus \hat{\mathbf{u}}_{1,e}^{2j-2}\right), L_{n/2}^{(j)}\left(\mathbf{y}_{n/2+1}^n, \hat{\mathbf{u}}_{1,e}^{2j-2}\right), \hat{u}_{2j-1}\right) \quad (5)$$

for $1 \leq j \leq n/2$, where

$$F(x, y) = 2 \tanh^{-1}(\tanh(x/2) \tanh(y/2)),$$

$$G(x, y, u) \triangleq (-1)^u x + y,$$

$\hat{\mathbf{u}}_{1,o}^i$ and $\hat{\mathbf{u}}_{1,e}^i$ are subvectors of $\hat{\mathbf{u}}_1^i$ with odd and even indices respectively. $L_1^{(1)}(r_i) \triangleq \ln \frac{W(r_i|0)}{W(r_i|1)}$ is the initial channel metric and \hat{u}_{2j-1} is the modulo-2 partial sum of previously decoded bits.

Similar to BP, the min-sum approximation can also be employed to reduce the complexity of (4):

$$F(x, y) \approx \text{sign}(x) \text{sign}(y) \min(|x|, |y|). \quad (6)$$

C. Density Evolution

The BP process can be analyzed by density evolution. Assume that $\mathbf{x} = \{x_1, \dots, x_n\} \in \{0, 1\}^n$ are transmitted through binary memoryless symmetric (BMS) channels $\mathbf{W} = \{W_1, \dots, W_n\}$, and $\mathbf{y} = \{y_1, \dots, y_n\}$ are received signals. Let

$$L(y_i) = \ln \frac{p(x_i = 0 | y_i)}{p(x_i = 1 | y_i)}$$

denote the corresponding LLR of y_i , and c_i be the density of $L(y_i)$ conditioned on $x_i = 0$. We call c_i the L -density of y_i . Then $c_i \in \mathcal{X}$ is a symmetric probability measure, where \mathcal{X} is a convex subset of symmetric probability measures [24]. The L -density of $m_{\alpha \rightarrow i}$ and $m_{i \rightarrow \alpha}$ are denoted by $c_{(\alpha, i)}$ and $c_{(i, \alpha)}$, respectively. The entropy function of L -density is the linear functional defined by

$$H(c) \triangleq \int_{-\infty}^{+\infty} c(y) \log_2(1 + e^{-y}) dy.$$

The convolution operations on the variable node and check node can be denoted by two binary operators \otimes and \boxtimes , respectively. For L -density c_1, c_2 , and any Borel set $E \subset \overline{\mathbb{R}}$, define

$$(c_1 \otimes c_2)(E) \triangleq \int_{\overline{\mathbb{R}}} c_1(E - \alpha) c_2(d\alpha),$$

$$(c_1 \boxtimes c_2)(E) \triangleq \int_{\overline{\mathbb{R}}} c_1 \left(2 \tanh^{-1} \left(\frac{\tanh\left(\frac{E}{2}\right)}{\tanh\left(\frac{\alpha}{2}\right)} \right) \right) c_2(d\alpha),$$

where $\int_{\overline{\mathbb{R}}} f(\alpha) c(d\alpha)$ is the Lebesgue integral with respect to probability measure c on extended real numbers $\overline{\mathbb{R}}$.

If the factor graph is cycle-free, then the update rule in (1), (2) can be written in the form of L -density

$$\begin{aligned} c_{(i, \alpha)}^{(l)} &= c_i \otimes \left(\otimes_{h \in N(i) \setminus \alpha} c_{(h, i)}^{(l-1)} \right), \\ c_{(\alpha, i)}^{(l)} &= \boxtimes_{j \in N(\alpha) \setminus i} c_{(j, \alpha)}^{(l-1)}. \end{aligned}$$

In order to analyze how the messages evolve in the decoding process, we introduce the following definitions and properties about L -density in [25].

Definition 1. For L -density c and $f : [0, 1] \rightarrow \mathbb{R}$, define

$$I_f(c) \triangleq \int_{\overline{\mathbb{R}}} f \left(\left| \tanh \left(\frac{\alpha}{2} \right) \right| \right) c(d\alpha).$$

We call c_1 is degraded with respect to c_2 (denoted by $c_1 \succeq c_2$), if $I_f(c_1) \geq I_f(c_2)$ for all concave non-increasing f . Furthermore, c_1 is said to be strictly degraded with respect to c_2 (denoted by $c_1 \succ c_2$) if $c_1 \succeq c_2$ and $c_1 \neq c_2$.

Degradation defines a partial order on the space of symmetric probability measures, with the greatest element Δ_0 and the least element Δ_∞ . Thus we have

$$c \succ \Delta_\infty \text{ if } c \neq \Delta_\infty, \text{ and } c \prec \Delta_0 \text{ if } c \neq \Delta_0.$$

The following proposition will be used in subsequent discussions.

Proposition 1. *Suppose $x_1, x_2, x_3, x'_1, x'_2 \in \mathcal{X}$.*

i) If $x_1 \succeq x_2$, then

$$x_1 \otimes x_3 \succeq x_2 \otimes x_3, \quad \text{for all } x_3 \in \mathcal{X},$$

$$x_1 \boxtimes x_3 \succeq x_2 \boxtimes x_3, \quad \text{for all } x_3 \in \mathcal{X}.$$

ii) If $x_1 \succ x_2$, then

$$H(x_1) > H(x_2).$$

iii)

$$H(x_1 \otimes x_2) + H(x_1 \boxtimes x_2) = H(x_1) + H(x_2).$$

iv) If $y_1 = x'_1 - x_1, y_2 = x'_2 - x_2$ with $x'_1 \succeq x_1, x'_2 \succeq x_2$, then

$$H(y_1 \boxtimes y_2) \leq 0, \quad H(y_1 \otimes y_2) \geq 0.$$

More properties about L-density and the entropy of symmetric measures can be found in [25] and chapter 4 of [24].

D. Bethe free energy

The BP algorithm plays an important role in decoding and even gives surprisingly good approximate results for graphical models with cycles [26]. The notion that fixed points of BP correspond to the extrema of the Bethe free energy is an essential step in the theoretical understanding of this success [27]. This subsection introduces the concept of Bethe free energy for subsequent variations based on it.

Let $i \in [1, n]$ and $\alpha \in [1, m]$ index the variable nodes and the check nodes in a factor graph, respectively. Assume that $\mathbf{x} = \{x_1, \dots, x_n\} \in \{0, 1\}^n$ is transmitted through BMS channel $\mathbf{W} = \{W_1, \dots, W_n\}$, and $\mathbf{y} = \{y_1, \dots, y_n\}$ is received signal. The MAP decoding is based on the following conditional density function

$$p(x_1, \dots, x_n | y_1, \dots, y_n) = \frac{\prod_1^n f_i(x_i) \prod_1^m f_\alpha(\mathbf{x}_\alpha)}{Z},$$

where $f_i(x_i) = W_i(y_i | x_i)$ is the channel transition probability, $f_\alpha(\mathbf{x}_\alpha) = I(\oplus \mathbf{x}_\alpha = 0)$ is the indicator function of whether check node α holds, $\mathbf{x}_\alpha = \{x_i, i \in N(\alpha)\}$, and Z is the partition function.

Since the complexity of MAP decoding through $\arg \max_{\mathbf{x} \in \mathcal{C}} p(x_1, \dots, x_n | y_1, \dots, y_n)$ is exponential, we need to find a density function to approximate p . Chapter 14 of [28] shows that if the factor graph is cycle-free, then we have the exact formula

$$p(\mathbf{x}) = \frac{\prod_{\alpha} p_{\alpha}(\mathbf{x}_{\alpha})}{\prod_i p_i(x_i)^{d_i-1}},$$

where d_i is the degree of variable node i , and p_i, p_{α} are marginal density functions. Hence we consider

$$b \in \mathfrak{M} = \left\{ \frac{\prod_{\alpha} b_{\alpha}(\mathbf{x}_{\alpha})}{\prod_i b_i(x_i)^{d_i-1}} \mid b_i(x_i) = \sum_{\mathbf{x}_{\alpha} \setminus x_i} b_{\alpha}(\mathbf{x}_{\alpha}) \right\}.$$

The Bethe free energy

$$F(b) \triangleq U_{\text{bethe}}(b) - H_{\text{bethe}}(b) = -\ln Z + D(b||p),$$

characterizes the distance between b and p , where

$$U_{\text{bethe}}(b) = -\sum_{\alpha=1}^m \sum_{\mathbf{x}_{\alpha}} b_{\alpha}(\mathbf{x}_{\alpha}) \ln f_{\alpha}(\mathbf{x}_{\alpha}) - \sum_{i=1}^n \sum_{x_i} b_i(x_i) \ln f_i(x_i),$$

$$H_{\text{bethe}}(b) = -\sum_{\alpha=1}^m \sum_{\mathbf{x}_{\alpha}} b_{\alpha}(\mathbf{x}_{\alpha}) \ln b_{\alpha}(\mathbf{x}_{\alpha}) + \sum_{i=1}^n (d_i - 1) \sum_{x_i} b_i(x_i) \ln b_i(x_i),$$

and

$$D(b||p) = \sum_{\mathbf{x} \in \{0,1\}^n} b(\mathbf{x}) \log \frac{b(\mathbf{x})}{p(\mathbf{x})}$$

is the relative entropy (Kullback-Leibler divergence). Hence it can be used to measure the gap between the density obtained by BP decoding and the MAP decoding result. For a fixed channel and coding scheme, i.e., fixed p , “ $-\ln Z$ ” is a constant, which enables us to observe $D(b||p)$ through Bethe free energy.

By the Lagrange multiplier method, we form the Lagrange multipliers γ_{α} and γ_i for the normalization constraints, $\lambda_{(\alpha i)}(x_i)$ for the marginalization constraints to find the stationary point of $F(b)$. We thus construct a Lagrangian of the below form

$$\begin{aligned} L = F &+ \sum_{\alpha=1}^m \gamma_{\alpha} \left[\sum_{\mathbf{x}_{\alpha}} b_{\alpha}(\mathbf{x}_{\alpha}) - 1 \right] + \sum_{i=1}^n \gamma_i \left[\sum_{x_i} b_i(x_i) - 1 \right] \\ &+ \sum_{i=1}^n \sum_{\alpha \in N(i)} \sum_{x_i} \lambda_{\alpha i}(x_i) \left[b_i(x_i) - \sum_{\mathbf{x}_{\alpha} \setminus x_i} b_{\alpha}(\mathbf{x}_{\alpha}) \right]. \end{aligned}$$

Setting the derivatives of the Lagrangian with respect to the Lagrange multipliers equal to zero gives back the equality constraints. Setting the derivatives of the Lagrangian with respect to $\{b_\alpha(x_\alpha), b_i(x_i)\}$ equal to zero gives the equations

$$\hat{b}_\alpha(\mathbf{x}_\alpha) \propto f_\alpha(\mathbf{x}_\alpha) \exp \left[\sum_{i \in N(\alpha)} \lambda_{\alpha i}(x_i) \right],$$

and

$$\hat{b}_i(x_i) \propto \exp \left[\frac{1}{d_i - 1} \left(-\ln f_i(x_i) + \sum_{a \in N(i)} \lambda_{ai}(x_i) \right) \right].$$

Let

$$\lambda_{\alpha i}(x_i) = \ln p_{i \rightarrow \alpha}(x_i) = \ln \left(f_i(x_i) \prod_{h \in N(i) \setminus \alpha} p_{h \rightarrow i}(x_i) \right), \quad (7)$$

then we have

$$\hat{b}_\alpha(\mathbf{x}_\alpha) \propto f_\alpha(\mathbf{x}_\alpha) \prod_{i \in N(\alpha)} p_{i \rightarrow \alpha}(x_i), \quad (8)$$

and

$$\hat{b}_i(x_i) \propto f_i(x_i) \prod_{\alpha \in N(i)} p_{\alpha \rightarrow i}(x_i). \quad (9)$$

We obtain the fixed-point equations of the BP algorithm from (8), (9), and the marginalization and normalization constraints [26]. Then we can change the variables from $\{b_\alpha(\mathbf{x}_\alpha), b_i(x_i)\}$ to $\underline{p} = \{p_{i \rightarrow \alpha}, p_{\alpha \rightarrow i}\}$ at the BP fixed point,

$$F_*(\underline{p}) = - \left(\sum_{\alpha} \mathbb{F}_\alpha(\underline{p}) + \sum_i \mathbb{F}_i(\underline{p}) - \sum_{(i, \alpha)} \mathbb{F}_{i\alpha}(\underline{p}) \right),$$

where

$$\mathbb{F}_\alpha(\underline{p}) = \ln \left[\sum_{\mathbf{x}_\alpha} f_\alpha(\mathbf{x}_\alpha) \prod_{j \in N(\alpha)} p_{j \rightarrow \alpha}(x_j) \right],$$

$$\mathbb{F}_i(\underline{p}) = \ln \left[\sum_{x_i} f_i(x_i) \prod_{h \in N(i)} p_{h \rightarrow i}(x_i) \right],$$

$$\mathbb{F}_{i\alpha}(\underline{p}) = \ln \left[\sum_{x_i} p_{i \rightarrow \alpha}(x_i) p_{\alpha \rightarrow i}(x_i) \right].$$

Since the channel is BMS, we send all-zero codeword and take the expectation over the channel noises, then we can get the expectation of Bethe free energy with respect to the channel output in a cycle-free factor graph,

$$\begin{aligned}
E_{\mathbf{y}}(F_*(\underline{p})) = & -\left\{ \sum_i H(c_i \circledast (\circledast_{\alpha \in N(i)} c_{(\alpha,i)})) + \sum_{\alpha} \sum_{i \in N(\alpha)} H(c_{(i,\alpha)}) \right. \\
& \left. - \sum_{\alpha} H(\circledast_{i \in N(\alpha)} c_{(i,\alpha)}) - \sum_{(i,\alpha)} H(c_{(i,\alpha)} \circledast c_{(\alpha,i)}) \right\} + \sum_i H(c_i),
\end{aligned} \tag{10}$$

where $\mathbf{c} = (c_1, \dots, c_n)$ is the L -density of channel message, $c_{(\alpha,i)}$ and $c_{(i,\alpha)}$ are the L -density of $m_{\alpha \rightarrow i}$ and $m_{i \rightarrow \alpha}$ on the BP fixed point.

The expectation of $E_{\mathbf{y}}(F_*(\underline{p}))$ with respect to the code ensemble (factor graphs with the same degree distribution) is the potential functional of LDPC ensemble in [25]. Correspondingly, our study will focus on the factor graph of a specific code in the next section.

III. CHARACTERIZATION OF DECODING EFFICIENCY

To establish an efficiency analysis, we need to explore the internal decoding process rather than focusing on the final decoding result only. Similar to the SNR-BLER paradigm, we characterize the decoding efficiency along two dimensions. Instead of the SNR-BLER curve, we adopt the *number of messages passed (NMP)* and *Gap to maximum A Posteriori (GAP)* to measure complexity and performance, respectively.

A. Number of messages passed (NMP) as the complexity metric (x-axis)

There are many ways to measure decoding complexity. The common ones are as follows. (1) The computational complexity in terms of the number of mathematical operations is the most commonly used. But it differs significantly across implementations [29]–[31]. (2) Tree search based algorithms, such as Fano decoding, consider the number of nodes visited. But this metric is difficult to be generalized to other algorithms. (3) For belief-propagation-based algorithms, the number of messages passed serves our purpose. First, it applies to a wide range of polar and LDPC decoding algorithms; second, the complexity of different algorithms can be aligned; third, it is independent of hardware implementation.

In [19], B. Smith et al. roughly count the number of messages passed as the number of edges in the factor graph multiplied by the number of iterations. If we only discuss the decoding of LDPC codes, this calculation method would be sufficient. However, if we want to have a fine-grained observation of the decoding process, we need a counting method that zooms in on each edge. The number of messages passed in this work is counted as follows. We define the V2C or C2V message passing on a directed edge as a unit of complexity. In the min-sum

algorithm, each C2V and V2C message passing have similar computational complexity. We can get all the updated C2V messages of a check node by $2d_c - 3$ comparison operations, where d_c is the check node degree. The average number of comparison operations required for any C2V message passing is less than 2. This property can also be achieved in the V2C message. We add up all the LLR values passed to the variable node and subtract the corresponding message when passing to the check node.

For LDPC codes, the arrowheaded line from c_1 to v_1 in Fig. 2(a) is an example of C2V message. We can obtain all the LLRs from c_1 to adjacent nodes by finding the two smallest values of $|m_{v_i \rightarrow c_1}|$ ($i \in (1, 4)$), and count the amount of floating-point computation required for each edge as shown in the first row of Table I. The V2C message passing is shown in Fig. 2(b), and its complexity can be analyzed in a similar way.

For polar codes, the factor graph is equivalent to a bipartite graph as shown in Fig. 2(c,d). Hence the same rules to measure complexity can be applied to the C2V or V2C update in polar codes. Specifically, the F function in (4) is a C2V update of a degree-3 check node, and the G function in (5) is a V2C update of a degree-2 variable node. The required computation is shown in the last two rows of Table I. Notice that we do not contain hard messages in the polar code factor graph when considering messages passed. This is in accordance with the characteristics of the SC decoding algorithm. Since the complex of a Boolean or assignment operation is negligible compared to a floating-point operation, we can assume that a hard decision removes a node (and its incident edges) from the factor graph. This complexity model is more consistent with the actual cost. At the same time, if we run the soft cancellation (SCAN) or BP algorithm on the polar factor graph, each edge updating that involves a floating-point operation will still be counted as a message passed.

TABLE I
FLOATING-POINT COMPUTATION OF EACH TYPE OF MESSAGE PASSING UNDER MIN-SUM ALGORITHM.

| | Addition | Subtraction | Comparison |
|-----------|----------|-------------|---------------------|
| LDPC C2V | 0 | 0 | $2 - \frac{3}{d_c}$ |
| LDPC V2C | 1 | 1 | 0 |
| Polar C2V | 0 | 0 | 1 |
| Polar V2C | 1 | 0 | 0 |

¹ d_c denotes the degree of check node.

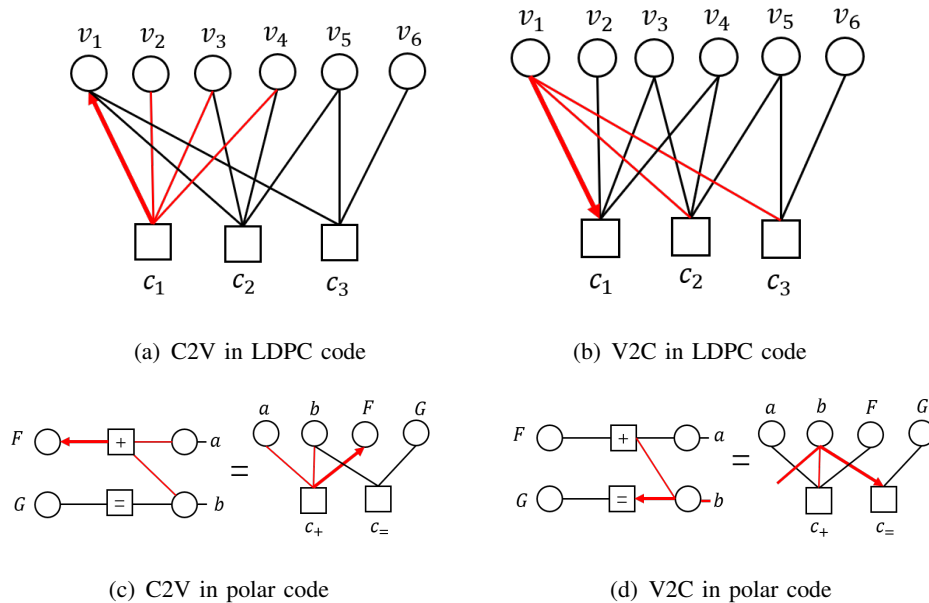


Fig. 2. Four types of message passing in LDPC and polar codes.

Given the above analyses, we find that different types of message passing involve similar amount of computation, which allows us to use NMP as a simplified measure of complexity. The NMP does not capture every detail, but provides a high-level abstraction of the complexity model for message-passing decoding algorithms.

B. Gap to maximum A Posteriori (GAP) as the performance metric (y-axis)

In this subsection, we elaborate a metric to track the convergence process as messages are passed along the edges. Many parameters can be used for this purpose. Naturally, one would consider the BLER and the BER. However, the changes of these parameters are observable only at the final decoding stage. This approach fails to track the effect of early-stage messages passed. An alternative metric is the statistical distance between an intermediate estimate and the maximum *a posteriori* estimate of the received codeword. Similar metrics like Bethe free energy have been applied to prove the threshold saturation for spatially-coupled LDPC codes [25]. The potential functional in [25] is more of a qualitative analysis to determine whether BP decoding will converge to a fixed point, but this work provides a quantitative analysis to track the behavior of BP decoding after passed each message until convergence. Rather than the original definition of Bethe free energy or the result by averaging over the code ensemble in [25], we consider a potential functional that results from averaging Bethe free energy over the channel

realizations. Since we no longer average over the code ensemble, we are able to consider the decoding process of a specific code or even a specific factor graph. This will be demonstrated shortly.

First we introduce the variation from the original definition of Bethe free energy to the proposed GAP potential functional. Recall the expectation of Bethe free energy with respect to the channel output

$$\begin{aligned} E_y(F_*(\underline{p})) &= -\left\{ \sum_i H\left(c_i \otimes \left(\otimes_{\alpha \in N(i)} c_{(\alpha,i)}\right)\right) \right. \\ &\quad + \sum_{\alpha} \sum_{i \in N(\alpha)} H\left(c_{(i,\alpha)}\right) - \sum_{\alpha} H\left(\boxtimes_{i \in N(\alpha)} c_{(i,\alpha)}\right) \\ &\quad \left. - \sum_{(i,\alpha)} H\left(c_{(i,\alpha)} \otimes c_{(\alpha,i)}\right)\right\} + \sum_i H(c_i). \end{aligned}$$

This formula focuses on $c_{(\alpha,i)}$ and $c_{(i,\alpha)}$, the convergence L -densities on the BP fixed point. To characterize the decoding process, we find that even if \underline{p} does not satisfy the fixed-point equation, $F_*(\underline{p})$ is still computable and its stationary point is a BP fixed point. Hence we can expand the domain of the variables $c_{(i,\alpha)}$ and $c_{(\alpha,i)}$ in $E_y(F_*(\underline{p}))$ from the BP fixed point to the whole decoding process by adding the number of messages passed as a new variable, and remove the terms which do not change with the decoding process. Based on such a generalization, we define a potential functional to track the message passing process.

Definition 2. *The gap to maximum a posteriori (GAP) is the potential functional, $U : \mathcal{X} \times \mathbb{N} \rightarrow \mathbb{R}$, of the number of messages passed t and channel messages with L -density $\mathbf{c} = (c_1, \dots, c_N)$*

$$\begin{aligned} U(\mathbf{c}, t) &\triangleq -\frac{1}{N} \left\{ \sum_i H\left(c_i \otimes \left(\otimes_{\alpha \in N(i)} c_{(\alpha,i)}^{(t)}\right)\right) + \sum_{\alpha} \sum_{i \in N(\alpha)} H\left(c_{(i,\alpha)}^{(t)}\right) \right. \\ &\quad \left. - \sum_{\alpha} H\left(\boxtimes_{i \in N(\alpha)} c_{(i,\alpha)}^{(t)}\right) - \sum_{(i,\alpha)} H\left(c_{(i,\alpha)}^{(t)} \otimes c_{(\alpha,i)}^{(t)}\right) \right\}. \end{aligned} \tag{11}$$

The initial value and update rule are given as follows.

$$\begin{aligned} c_{(\alpha,i)}^{(0)} &= c_{(i,\alpha)}^{(0)} = \Delta_0, \\ c_{(\alpha,i)}^{(t)} &= \boxtimes_{j \in N(\alpha) \setminus i} c_{(j,\alpha)}^{(t-1)}, \end{aligned}$$

and

$$c_{(i,\alpha)}^{(t)} = c_i \circledast \left(\circledast_{h \in N(i) \setminus \alpha} c_{(h,i)}^{(t-1)} \right).$$

Specifically, when i represents an information bit or frozen bit in polar codes, we have $c_{(i,\alpha)}^{(t)} = \Delta_\infty$.

Remark. In Definition 2, we assume that the factor graph G and scheduling policy S are fixed. Strictly, $U(\mathbf{c}, t)$ should be written as $U(\mathbf{c}, t, G, S)$, otherwise we do not have $U(\mathbf{c}, t) = U(\mathbf{c}, t')$ when $t = t'$. The factor graph is associated with the coding scheme, and the scheduling policy can be described as follows.

Definition 3 (Scheduling policy). If we label each directed edge in a factor graph from 1 to k , then a scheduling policy can be denoted by a sequence $S = \{s_1, \dots, s_p\}$, where $p \in \mathbb{N}$ and $s_i \in [1, k]$ ($1 \leq i \leq p$).

The scheduling policy S indicates which edge should be updated at each step. Compared with the description of layered BP or other previous studies, this definition gives us a better characterization of scheduling policy. By viewing decoding as a dynamic process, we can zoom in to observe the differences of $U(\mathbf{c}, t)$ between factor graphs and the efficiency of scheduling policies. The comparison results can be found in Section IV and V.

C. Monotonicity and boundedness

Next, we will discuss the monotonicity and boundedness of $U(\mathbf{c}, t)$ and reveal its relationship to message passing. Consider the communication over a BMS channel under the all-zero codeword assumption. Let $X = \{x_1, \dots, x_N\} \in \{0, 1\}^N$ and $Y = \{y_1, \dots, y_N\} \in \mathbb{R}^N$ denote the input and output of the BMS channel respectively, $\mathbf{c} = (c_1, \dots, c_N)$ be the L -density of the output, and R be the code rate.

Theorem 2. Assume that the fixed factor graph G is cycle-free, then for any scheduling policy S and $t \geq 1$, $U(\mathbf{c}, t)$ is monotonic decreasing with t . The upper bound of $U(\mathbf{c}, t)$ is $1 - R - \frac{1}{N} \sum_{i=1}^N H(c_i)$ and the lower bound is $-\frac{1}{N} H(X|Y)$.

The following propositions and lemmas will accomplish the proof of Theorem 2 and help us to understand the meaning of $U(\mathbf{c}, t)$ in the decoding process.

Proposition 3 (Initial value). *The initial value $U(\mathbf{c}, 0)$ of a fixed factor graph is $1 - R - \frac{1}{N} \sum_i H(c_i)$.*

This proposition holds clearly by substituting $c_{(\alpha,i)}^{(0)} = c_{(i,\alpha)}^{(0)} = \Delta_0$ into the formula (11). We can find that the initial value is negatively correlated with channel entropy. A negative initial value indicates the code rate exceeds channel capacity.

Lemma 4. *Consider using a message-passing algorithm in a cycle-free factor graph. For any $t \geq 1$, the t -th message passing (C2V or V2C) satisfies $c_{\alpha,i}^{(t-1)} \succeq c_{\alpha,i}^{(t)}$ or $c_{i,\alpha}^{(t-1)} \succeq c_{i,\alpha}^{(t)}$.*

Proof. We use the induction method. For $t = 1$, if the first message passing is V2C, then we have $c_{i,\alpha}^{(1)} = c_i \preceq c_{i,\alpha}^{(0)}$; if the first message passing is C2V, then we have $c_{\alpha,i}^{(1)} = c_{\alpha,i}^{(0)}$. We assume that this conclusion holds if $t \leq k$ and consider $t = k + 1$. If i is associated with an information bit or frozen bit in the polar code factor graph, then we get

$$c_{(i,\alpha)}^{(k+1)} = \Delta_\infty \preceq c_{(i,\alpha)}^{(k)},$$

else

$$\begin{aligned} c_{i,\alpha}^{(k+1)} &= c_i \otimes \left(\otimes_{h \in N(i) \setminus \alpha} c_{(h,i)}^{(k)} \right) \\ &\preceq c_i \otimes \left(\otimes_{h \in N(i) \setminus \alpha} c_{(h,i)}^{(k-1)} \right) \\ &= c_{i,\alpha}^{(k)}. \end{aligned}$$

We can similarly get $c_{\alpha,i}^{(k+1)} \preceq c_{\alpha,i}^{(k)}$ which completes our proof. \square

Proposition 5 (Monotonic decreasing). *For any scheduling policy S and $t \geq 1$, the t -th message passing (C2V or V2C) satisfies $U(\mathbf{c}, t) \leq U(\mathbf{c}, t - 1)$.*

Proof. We discuss the two types of message passing separately. If the t -th message passing is C2V, that is, there is a $c_{\alpha,i}^{(t-1)}$ updated to $c_{\alpha,i}^{(t)}$, then we can only consider the change related to the edge (α, i) . Notice that the message update only affects the first and the last terms of $U(\mathbf{c}, t - 1)$,

hence we have

$$\begin{aligned}
& NU(\mathbf{c}, t) - NU(\mathbf{c}, t - 1) \\
&= -H\left(c_{\alpha,i}^{(t)} \otimes c_i \otimes \left(\otimes_{h \in N(i) \setminus \alpha} c_{h,i}^{(t-1)}\right)\right) \\
&+ H\left(c_{\alpha,i}^{(t-1)} \otimes c_i \otimes \left(\otimes_{h \in N(i) \setminus \alpha} c_{h,i}^{(t-1)}\right)\right) \\
&+ H\left(c_{\alpha,i}^{(t)} \otimes c_{i,\alpha}^{(t-1)}\right) - H\left(c_{\alpha,i}^{(t-1)} \otimes c_{i,\alpha}^{(t-1)}\right) \\
&= H\left(\left(c_{\alpha,i}^{(t-1)} - c_{\alpha,i}^{(t)}\right) \otimes c_i \otimes \left(\otimes_{h \in N(i) \setminus \alpha} c_{h,i}^{(t-1)}\right)\right) \\
&- H\left(\left(c_{\alpha,i}^{(t-1)} - c_{\alpha,i}^{(t)}\right) \otimes c_{i,\alpha}^{(t-1)}\right) \\
&= H\left(\left(c_{\alpha,i}^{(t-1)} - c_{\alpha,i}^{(t)}\right) \otimes \left(c_i \otimes \left(\otimes_{h \in N(i) \setminus \alpha} c_{h,i}^{(t-1)}\right) - c_{i,\alpha}^{(t-1)}\right)\right).
\end{aligned}$$

By Lemma 4, we have $c_{\alpha,i}^{(t-1)} \succeq c_{\alpha,i}^{(t)}$. Since $H(x_1 \otimes x_2) \geq H(x_3 \otimes x_2)$ when $x_1 \succeq x_3$, we have $c_{i,\alpha}^{(t-1)} = c_i \otimes \left(\otimes_{h \in N(i) \setminus \alpha} c_{h,i}^{(t-2)}\right) \succeq c_i \otimes \left(\otimes_{h \in N(i) \setminus \alpha} c_{h,i}^{(t-1)}\right)$, hence $U(\mathbf{c}, t) - U(\mathbf{c}, t - 1) \leq 0$.

If the t -th message passing is V2C, using $H(x_1 \boxtimes x_2) = H(x_1) + H(x_2) - H(x_1 \otimes x_2)$, then we can similarly get

$$\begin{aligned}
& U(\mathbf{c}, t) - U(\mathbf{c}, t - 1) \\
&= \frac{1}{N} H\left(\left(c_{i,\alpha}^{(t-1)} - c_{i,\alpha}^{(t)}\right) \otimes \left(\left(\boxtimes_{j \in N(\alpha) \setminus i} c_{j,\alpha}^{(t-1)}\right) - c_{\alpha,i}^{(t-1)}\right)\right) \\
&\leq 0.
\end{aligned}$$

□

We can get a sufficient and necessary condition for $U(\mathbf{c}, t)$ to be strictly decreasing.

Corollary 6. *If the t -th message passing is C2V, then $U(\mathbf{c}, t) < U(\mathbf{c}, t - 1)$ if and only if*

$$c_{\alpha,i}^{(t-1)} \succ c_{\alpha,i}^{(t)} \text{ and } c_{i,\alpha}^{(t-1)} \succ c_i \otimes \left(\otimes_{h \in N(i) \setminus \alpha} c_{h,i}^{(t-1)}\right).$$

If the t -th message passing is V2C, then $U(\mathbf{c}, t) < U(\mathbf{c}, t - 1)$ if and only if

$$c_{i,\alpha}^{(t-1)} \succ c_{i,\alpha}^{(t)} \text{ and } c_{\alpha,i}^{(t-1)} \succ \left(\boxtimes_{j \in N(\alpha) \setminus i} c_{j,\alpha}^{(t-1)}\right).$$

Corollary 6 implies that “better” messages may not lead to an instant decrease of the potential functional. The “delay” of message update is necessary. The potential functional of the SC algorithm in the polar code factor graph characterizes this phenomenon.

Corollary 7. *In the SC decoding algorithm, $U(\mathbf{c}, t)$ decreases if and only if the updated edge is incident with a frozen bit node.*

Since only frozen bits can offer messages with

$$c_{i,\alpha}^{(t-1)} \succ c_i \circledast \left(\circledast_{h \in N(i) \setminus \alpha} c_{h,i}^{(t-1)} \right),$$

by Corollary 6, we can get this property which leads to many interesting observations to be shown in the next section.

Then we introduce the conditional entropy of tree code, and it corresponds to the lower bound of $U(\mathbf{c}, t)$.

Lemma 8 [3]. *If the factor graph is cycle-free, then*

$$\begin{aligned} H(X|Y) &= \sum_i H(c_i \circledast (\circledast_{\alpha \in N(i)} c_{(\alpha,i)})) \\ &+ \sum_{\alpha} \sum_{i \in N(\alpha)} H(c_{(i,\alpha)}) - \sum_{\alpha} H(\circledast_{i \in N(\alpha)} c_{(i,\alpha)}) \\ &- \sum_{(i,\alpha)} H(c_{(i,\alpha)} \circledast c_{(\alpha,i)}). \end{aligned}$$

Proposition 9 (Lower bound). *For fixed cycle-free factor graph G and any scheduling policy, we have $U(\mathbf{c}, t) \geq -\frac{1}{N}H(X|Y)$.*

Proof. From Corollary 6, we can find that $U(\mathbf{c}, t)$ in the BP fixed point is minimal. At the same time, by Lemma 8, the minimal value is $-\frac{1}{N}H(X|Y)$. \square

During the decoding process, the marginalization constraints are not satisfied. Hence we can not regard $U(\mathbf{c}, t)$ as a Kullback-Leibler divergence between two densities. But it reflects the process in which the BP decoding results are constantly approaching the density of the MAP decoding. We can track the changing process of $U(\mathbf{c}, t)$ with respect to its gap to $-\frac{1}{N}H(X|Y)$ (in most cases, we do not really need to know what the exact value is). The lower bound of $U(\mathbf{c}, t)$ implies that the BP decoder achieves the MAP decoding result and this result can be found in Chapter 15 of [28]. It also implies $U(\mathbf{c}, t) \rightarrow 0$ as $t \rightarrow \infty$ is the necessary condition of error-free decoding.

Before moving on to the next step, we clarify two approximations involved in the ‘‘NMP-GAP’’ model. The first is the approximation of the min-sum algorithm to the sum-product algorithm.

We analyze GAP under the sum-product algorithm but use the min-sum algorithm to ensure C2V messages have roughly equivalent complexity to the V2C messages. Wiberg shows that the sum-product and the min-sum algorithm are formally equivalent [32]. The second is the approximation of graphs with cycles to cycle-free graphs. Heskes shows that, in factor graphs with cycles, the BP fixed points in factor graphs with cycles are still the minima of the Bethe free energy [27]. As the code length goes to infinity, the LDPC factor graphs are asymptotically cycle-free [2]. For polar codes, the effects of cycles are not exhibited due to the scheduling and hard decisions in SC decoding. We will show in the subsequent sections that both approximations work for finite-length codes with cycles.

IV. DECODING EFFICIENCY ANALYSIS OF SEVERAL ALGORITHMS

In this section, we plot the “number of messages passed (NMP) versus the Gap to maximum *A Posteriori* (GAP)” curves of several algorithms through simulations and GA analysis under AWGN channel. The LDPC and polar codes construction follow 5G New Radio. We will introduce these “NMP-GAP” curves from four aspects: complexity, slope, convergence of decoding and analytical method.

In the following, we compare six decoding algorithms for polar and LDPC codes in terms of decoding efficiency:

- 1) Flooding BP decoding for LDPC codes;
- 2) Layered BP decoding for LDPC codes;
- 3) SC decoding for polar codes;
- 4) Simplified SC (SSC) decoding [33] for polar codes;
- 5) Soft cancellation (SCAN) decoding [34] for polar codes;
- 6) BP decoding [35] for polar codes.

A. Complexity

This subsection compares the complexities of the six algorithms and discusses the relationship between complexity and code length. Fig. 3 shows the simulation results of the six algorithms. At the same time, Fig. 4 shows the corresponding SNR-BLER curves as a reference. According to Fig. 4, we observe that these coding schemes have similar (or slightly different) performance, but we may not realize their contrasting complexity without observing Fig. 3. A key information missing in SNR-BLER curve is a quantitative measurement of the decoding complexity. For

many applications, we are more concerned about such a huge complexity difference than a modest BLER performance difference (for example, $< 0.5dB$). With the proposed paradigm, we are able to compare various decoding algorithms from a new perspective.

As shown in Fig. 3, the SSC and SC algorithms achieve high efficiency through proper scheduling. This explains why Polar SC/SSC can achieve terabit-per-second decoding. SCAN also has relatively low complexity. But the BP algorithm for polar codes, which runs on the same factor graph, has the lowest decoding efficiency among all schemes. However, the BP algorithm for LDPC codes incurs much less complexity than that of polar codes, thanks to the sparse factor graph. Still, both flooding-BP and layered-BP algorithms exhibit lower decoding efficiency than SC decoding.

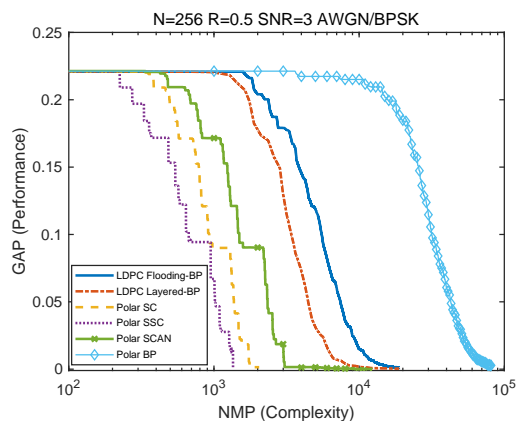


Fig. 3. The NMP-GAP curves obtained by simulations.

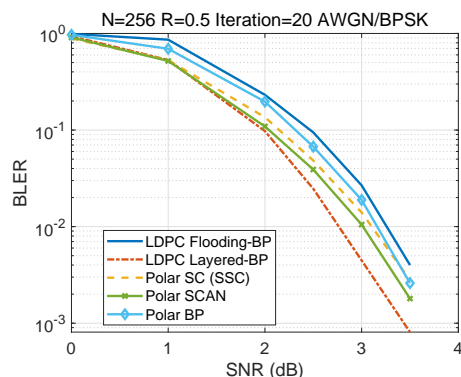


Fig. 4. The SNR-BLER curves obtained by simulations.

Next, we show that the asymptotic complexity is sometimes too coarse to compare decoding

algorithms fairly. Given a polar code with length N , the asymptotic complexities of the SC, SCAN and polar BP algorithm are $O(N \log N)$ [34], [35], and that of SSC is $O(N \log \log N)$ [36]–[38], while the complexities of BP algorithms in LDPC codes are generally considered $O(N)$ per iteration. Fig. 5 shows the NMP required for different code lengths. The NMP required in the SC decoder is $N \log N$, and SSC required is less (the actual number depends on the code used). SCAN and polar BP decoder’s NMP are $2 \times iter \times N \log N$, where $iter$ is the number of iterations. The NMP in layered-BP [39] and flooding-BP decoder is $2d \times iter \times N$, where d is the average degree of variable nodes. In particular, we note that polar BP and SC algorithms have the same asymptotic complexity, but their difference in terms of NMP can be two orders of magnitude. This reveals that, for polar codes, BP decoding requires much more messages passed than SC decoding to achieve the same decoding effect and should be considered less computationally efficient. From Fig. 3, we observe the decoding efficiency of layered BP is higher than flooding BP, as expected. These observations are consistent with the implementation cost in practice but cannot be revealed by asymptotic complexity. The advantage of NMP over asymptotic complexity is that the former provides a higher resolution in observing the actual decoding complexity.

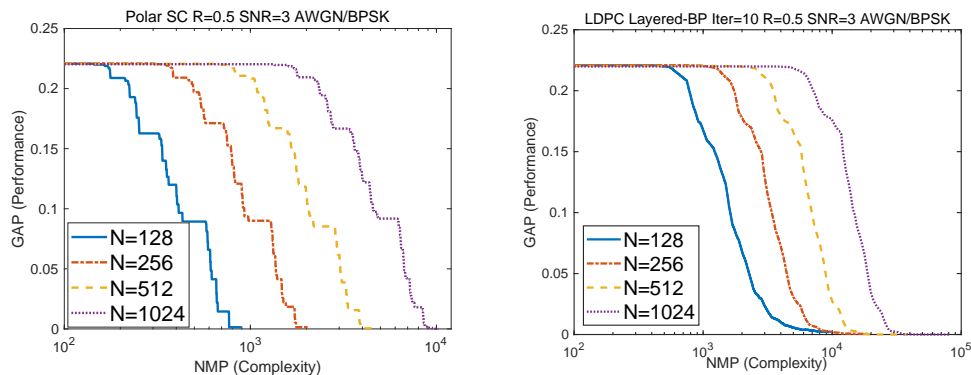


Fig. 5. The NMP-GAP curves with different code lengths.

The difference between SC and SSC algorithms is also worth to discuss. In this study, we consider four types of fast-decodable nodes, rate-0 (R0), rate-1 (R1), single parity check (SPC), and repetition (REP) [33]. When the decoder traverses to an R0 or R1 node, we only need to make some hard decisions. For an SPC node of length M , we need $M - 1$ times of comparison; for an REP node, we need $M - 1$ times of addition. We count the NMP of an SPC/REP node as $M - 1$. The efficiency of SSC has been captured by the “NMP-GAP” curves in Fig. 3. Note that

we do not discuss SCL decoding in this paper due to its list path management operations. For example, path extension, sorting, and pruning cannot be analyzed within the message-passing framework. We leave this as an interesting problem to solve.

B. Slope

The slope of the ‘‘NMP-GAP’’ curve is another property for us to observe the decoding efficiency. It is related to decoding algorithm, code length, code rate, and SNR. In Fig. 5, we find that the code length also affects the slope of the LDPC code. LDPC codes in shorter lengths have a smaller slope. To some extent, it reflects the inefficiency of LDPC codes with short lengths. The simulation results in Fig. 6 show that the BP algorithm is more efficient under higher SNR because it converges faster with fewer iterations. These observations may have been founded in previous studies, but they also demonstrate that our metrics well align with existing knowledge.

The complexity of polar code does not change with the SNR. The slope of the SC algorithm can be characterized by Theorem 2 and Corollary 7, which is well verified by the simulation results in Fig. 6.

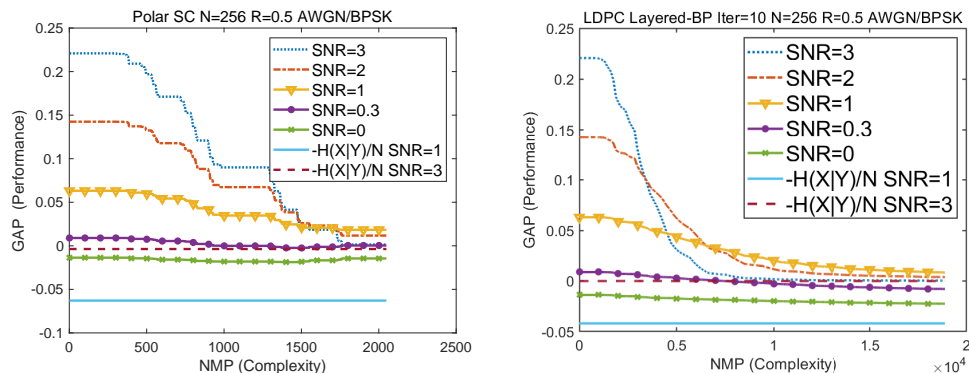


Fig. 6. NMP-GAP curves with different SNRs.

C. Convergence of decoding

In Fig. 6, the GAP curve at low SNR clearly crosses the X-axis, and these results are consistent with Proposition 3 and Proposition 9. When the code length is finite ($\frac{1}{N}H(X|Y)$ strictly large than zero), the GAP curve in the decoding process is not always nonnegative but remains the property that decreases monotonically with NMP. The GAP value being negative is not inconsistent with

the concept of distance. For most finite factor graphs, $H(X|Y)$ is an incalculable constant value. Hence we can regard $GAP + \frac{1}{N}H(X|Y)$ as a nonnegative statistic distance, and GAP is the part that is changing with decoding. Focusing on GAP enables us to accurately describe the decoding process without considering the incalculable conditional entropy in practical applications. The approximate values of $-\frac{1}{N}H(X|Y)$ at different SNRs are calculated through the sum of low-weight codewords and shown as the straight lines in Fig. 6. We use 3×10^6 lowest-weight polar codewords and about 4×10^{14} low-weight LDPC codewords.

Despite the simulation errors and the effect of cycles in the factor graph, the curves in this section are consistent with the theoretical convergence analysis. Through extensive simulations, we single out the following interesting observations as shown in Fig. 7. We obtain these curves from a single decoding attempt under a channel realization (it can be regarded as a channel that does not conform to the BMS hypothesis). When the first error of polar code occurs at an early stage (theoretically inadequately polarized), all subsequent bits will be affected by this error. The result is that the potential functional does not converge to the MAP decoding result but deviates from it. When the first error bit occurs in a later stage (theoretically fully polarized), the decoder will trust the incorrect bit with a large degree of confidence. Still, it only affects a few subsequent nodes, which leads to a result that most of the bits are the same as the MAP decoding. These are the two types of decoding failures for polar codes. The decoding process either diverges from the MAP results (the first case) or converges to it (the latter case).

By contrast, the decoding failures for LDPC codes fall into two situations: converging to a wrong result or oscillating between two results. When the error messages gradually become the consensus, the decoding result gets stuck at a wrong fixed point. In the oscillation case, given more iteration times, the decoding result may still stop on the correct one.

D. Analytical method

Alternative to the simulation-based approach, the change of $U(c, t)$ can also be evaluated analytically by Gaussian approximation [40]. We initialize the input of decoder by m_0 which is normally distributed with mean value $u_0 = \frac{2}{\sigma^2}$ and variance $2u_0$, where σ^2 is the variance of AWGN channel. The Gaussian approximation assumes that the V2C message $m_{i \rightarrow \alpha}$ or C2V message $m_{\alpha \rightarrow i}$ during the decoding process are normally distributed with the mean value $u_{i \rightarrow \alpha}$ and $u_{\alpha \rightarrow i}$, respectively. The update rule for V2C L-density's mean value is

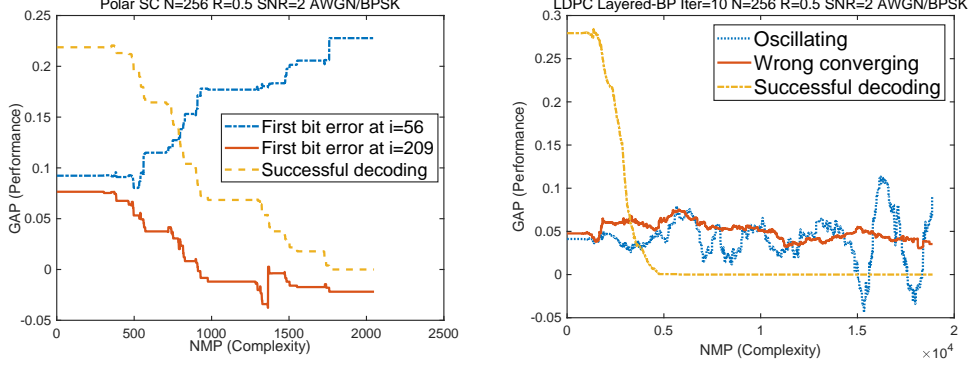


Fig. 7. Simulation results from individual decoding attempts.

$$u_{i \rightarrow \alpha} = u_0 + \sum_{h \in N(i) \setminus \alpha} u_{h \rightarrow i}, \quad (12)$$

and the update rule for C2V edge is

$$u_{\alpha \rightarrow i} = \varphi^{-1} \left\{ 1 - \prod_{j \in N(\alpha) \setminus i} [1 - \varphi(u_{j \rightarrow \alpha})] \right\}, \quad (13)$$

where

$$\varphi(x) = \begin{cases} 1 - \frac{1}{\sqrt{4\pi x}} \int_{\mathbb{R}} \tanh\left(\frac{u}{2}\right) e^{-\frac{(u-x)^2}{4x}} du, & x > 0, \\ 1, & x = 0. \end{cases} \quad (14)$$

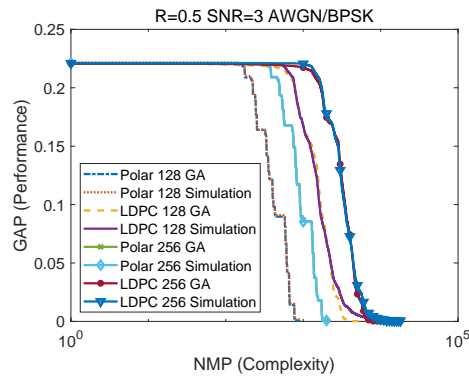


Fig. 8. Gaussian approximation and simulation results.

We approximate the “NMP-GAP” curve by the above updating rules. Fig. 8 shows that there are few deviations from the simulation results. We can employ analytical approaches to speed up the evaluations significantly.

V. APPLICATION

In this section, we apply the “NMP-GAP” paradigm to the scheduling policy design of LDPC codes. As discussed in the remark of Definition 2, the scheduling policy S can be regarded as a variable of GAP. We can obtain an optimization model of scheduling policy through it, that is, for a given number t_{max} , factor graph G and channel \mathbf{c}

$$\min U(\mathbf{c}, t, G, S) \quad (15)$$

$$\text{s.t. } t \leq t_{max}. \quad (16)$$

Section IV-D shows that the Gaussian approximation can well estimate the GAP calculation, which enables us to easily measure the change of GAP after any message passed. At the same time, most optimization methods including machine learning can be used in this optimization model. Different from the residual BP and other online (dynamic) scheduling algorithms [41], [42], scheduling based on “NMP-GAP” is off-line. Online scheduling needs to recalculate a new scheduling policy for each decoding attempt, which increases the latency and overall complexity. Off-line scheduling policy based on “NMP-GAP” only depends on the factor graph, which only needs to be executed once to obtain a fixed scheduling. Compared with the heuristic least-punctured highest-degree (LPHD) scheduling in [43], this optimization model has more room for further improvement. We design the following greedy algorithm as an example to illustrate the effectiveness of this model.

Algorithm 1 Greedy scheduling policy

// Initialization:

Set the factor graph G and $\mathbf{c} = \{c_1, \dots, c_n\}$ to initialize the GAP functional $U(\mathbf{c}, 0)$;

Set decode step $t = 0$, maximum decode step t_{max} and scheduling policy $S = \{\}$;

// Loop:

while $t \leq t_{max}$ **do**

1. For each check node $k \in \mathcal{C}$, calculate the change of GAP when we update its incident edges $a_k = \frac{1}{d_k}(U(\mathbf{c}, t) - U(\mathbf{c}, t + 2d_k))$, where d_k denotes the degree of k ;
2. Append $j = \arg \max_{k \in \mathcal{C}} a_k$ to S ;
3. Update incident edges of j and let $t = t + 2d_j$;

end while

Output S .

Considering the scheduling policy for protograph LDPC codes, we can bind the nodes which are copies of the same protograph node to reduce the search space. For the 5G LDPC codes, we compare the average NMP among the greedy algorithm, LPHD scheduling policy, and original layered algorithm. In the case of BLER being very close, the scheduling policy with lower NMP-GAP curve has higher efficiency. The simulation results of three scheduling policies and the average NMP are shown in Fig. 9 and Table II, respectively. The greedy scheduling policy is output by Algorithm 1 with SNR=2.5, and the simulation results show that this scheduling is still more efficient than others when SNR is lower than 2.5.

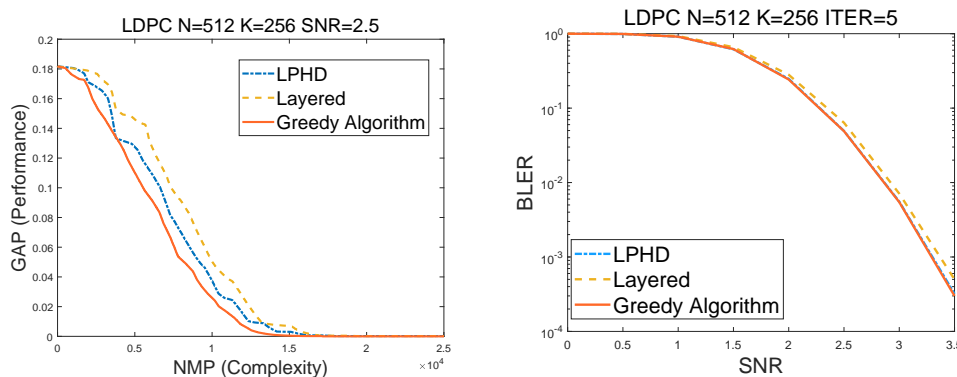


Fig. 9. NMP-GAP and SNR-BLER curves with different scheduling policy.

TABLE II
AVERAGE NMP OF 3 SCHEDULING POLICIES.

| SNR | 0.5 | 1 | 1.5 | 2 | 2.5 | 3 | 3.5 |
|------------------|----------|----------|----------|----------|----------|----------|----------|
| Layered | 9436.46 | 9393.98 | 9087.18 | 8219.29 | 6969.08 | 5860.47 | 5001.43 |
| LPHD | 9432.761 | 9344.18 | 8869.054 | 7776.445 | 6426.002 | 5312.973 | 4499.349 |
| Greedy Algorithm | 9430.799 | 9310.106 | 8756.131 | 7640.506 | 6411.519 | 5319.498 | 4513.586 |

¹ N=512, K=256, Maximum number of iterations=5.

VI. CONCLUSION

In this study, we present a model to measure the efficiency of several message-passing decoding algorithms. That is, measuring how many messages passed are required in order to achieve a certain gap from MAP decoding. Among many well-known decoding algorithms for polar and

LDPC codes, we find that SC decoding for polar codes exhibits the best decoding efficiency under the new paradigm, although it is conventionally labeled with moderate performance. We adopt the “NMP” to give an implementation-independent complexity measurement and the “GAP” to describe the decoding process in a high resolution. The “NMP-GAP” method provides insights into the design and evaluation of several decoding algorithms. It prompts us to rethink coding schemes from the “decoding efficiency” perspective, in addition to the “decoding performance” perspective.

REFERENCES

- [1] E. Arkan, “Channel polarization: A method for constructing capacity-achieving codes,” in *Proc. IEEE Int. Symp. Inf. Theory (ISIT)*, 2008, pp. 1173–1177.
- [2] T. Richardson, M. Shokrollahi, and R. L. Urbanke, “Design of capacity-approaching irregular low-density parity-check codes,” *IEEE Trans. Inf. Theory*, vol. 47, no. 2, pp. 619–637, 2001.
- [3] S. Kudekar, T. Richardson, and R. L. Urbanke, “Spatially coupled ensembles universally achieve capacity under belief propagation,” *IEEE Trans. Inf. Theory*, vol. 59, no. 12, pp. 7761–7813, 2013.
- [4] Y. Polyanskiy, *Channel coding: Non-asymptotic fundamental limits*. Ph. D. dissertation, Princeton Univ., 2010.
- [5] E. R. Berlekamp, *Algebraic Coding Theory*. McGraw-Hill, 1968.
- [6] M. Waldrop, “The chips are down for Moore’s law,” *Nat. News*, vol. 530, pp. 145–147, 01 2016.
- [7] A. Süral, E. G. Sezer, Y. Ertuğrul, O. Arkan, and E. Arıkan, “Terabits-per-second throughput for polar codes,” in *Proc. IEEE 30th Int. Symp. Pers. Indoor Mobile Radio Commun. (PIMRC)*, 2019, pp. 1–7.
- [8] A. Süral, E. G. Sezer, E. Kolağasıoğlu, V. Derudder, and K. Bertrand, “Tb/s polar successive cancellation decoder 16nm asic implementation,” *arXiv:2009.09388*, 2020.
- [9] J. Tong, X. Wang, Q. Zhang, H. Zhang, R. Li, J. Wang, and W. Tong, “Fast polar codes for terabits-per-second throughput communications,” *arXiv:2107.08600*, 2021.
- [10] N. Hussami, S. B. Korada, and R. Urbanke, “Performance of polar codes for channel and source coding,” in *Proc. IEEE Int. Symp. Inf. Theory (ISIT)*, 2009, pp. 1488–1492.
- [11] N. Goela, S. B. Korada, and M. Gastpar, “On LP decoding of polar codes,” in *Proc. IEEE Inf. Theory Workshop (ITW)*, 2010, pp. 1–5.
- [12] I. Tal and A. Vardy, “List decoding of polar codes,” *IEEE Trans. Inf. Theory*, vol. 61, no. 5, pp. 2213–2226, 2015.
- [13] K. Niu and K. Chen, “CRC-aided decoding of polar codes,” *IEEE Commun. Lett.*, vol. 16, no. 10, pp. 1668–1671, 2012.
- [14] J. Wozencraft and R. Kennedy, “Modulation and demodulation for probabilistic coding,” *IEEE Trans. Inf. Theory*, vol. 12, no. 3, pp. 291–297, 1966.
- [15] R. G. Gallager, *Information Theory and Reliable Communication*. New York: Wiley, 1968.
- [16] J. L. Massey, “Coding and modulation in digital communications,” in *Proc. Int. Zurich Sem. Digital Commun.*, 1974.
- [17] R. J. McEliece, “Are turbo-like codes effective on nonstandard channels?” *IEEE Trans. Inf. Theory Soc. Newsletter*, vol. 51, no. 4, pp. 1–8, 2001.
- [18] R. Gallager, “Low-density parity-check codes,” *IEEE Trans. Inf. Theory*, vol. 8, no. 1, pp. 21–28, 1962.
- [19] B. Smith, M. Ardakani, W. Yu, and F. R. Kschischang, “Design of irregular LDPC codes with optimized performance-complexity tradeoff,” *IEEE Trans. Commun.*, vol. 58, no. 2, pp. 489–499, 2010.

- [20] M. Fossorier, "Polar codes: Graph representation and duality," *IEEE Commun. Lett.*, vol. 19, no. 9, pp. 1484–1487, 2015.
- [21] R. Tanner, "A recursive approach to low complexity codes," *IEEE Transactions on Information Theory*, vol. 27, no. 5, pp. 533–547, 1981.
- [22] F. Kschischang, B. Frey, and H.-A. Loeliger, "Factor graphs and the sum-product algorithm," *IEEE Trans. Inf. Theory*, vol. 47, no. 2, pp. 498–519, 2001.
- [23] J. Chen, A. Dholakia, E. Eleftheriou, M. Fossorier, and X.-Y. Hu, "Reduced-complexity decoding of LDPC codes," *IEEE Trans. Commun.*, vol. 53, no. 8, pp. 1288–1299, 2005.
- [24] T. Richardson and R. Urbanke, *Modern Coding Theory*. Cambridge, U.K.: Cambridge Univ. Press, 2008.
- [25] S. Kumar, A. J. Young, N. Macris, and H. D. Pfister, "Threshold saturation for spatially coupled LDPC and LDGM codes on BMS channels," *IEEE Trans. Inf. Theory*, vol. 60, no. 12, pp. 7389–7415, 2014.
- [26] J. Yedidia, W. Freeman, and Y. Weiss, "Constructing free-energy approximations and generalized belief propagation algorithms," *IEEE Trans. Inf. Theory*, vol. 51, no. 7, pp. 2282–2312, 2005.
- [27] T. Heskes, "On the uniqueness of loopy belief propagation fixed points," *Neural Computation*, vol. 16, no. 11, pp. 2379–2413, 2004.
- [28] M. Mezard and A. Montanari, *Information, Physics, and Computation*. Oxford University Press, 2009.
- [29] C. G. Blake and F. R. Kschischang, "Upper and lower bounds on the computational complexity of polar encoding and decoding," *IEEE Trans. Inf. Theory*, vol. 65, no. 9, pp. 5656–5673, 2019.
- [30] H. Jeong and P. Grover, "Energy-adaptive codes," in *Proc. 53rd Annu. Allerton Conf. Commun., Control, Comput. (Allerton)*, 2015, pp. 132–139.
- [31] C. G. Blake and F. R. Kschischang, "On the VLSI energy complexity of LDPC decoder circuits," *IEEE Trans. Inf. Theory*, vol. 63, no. 5, pp. 2781–2795, 2017.
- [32] N. Wiberg, "Codes and decoding on general graphs," *Ph. D. dissertation, Linköping Univ. Sweden*, 1996.
- [33] A. Alamdar-Yazdi and F. R. Kschischang, "A simplified successive-cancellation decoder for polar codes," *IEEE Commun. Lett.*, vol. 15, no. 12, pp. 1378–1380, 2011.
- [34] U. U. Fayyaz and J. R. Barry, "Low-complexity soft-output decoding of polar codes," *IEEE J. Sel. Areas Commun.*, vol. 32, no. 5, pp. 958–966, 2014.
- [35] E. Arkan, "Polar codes: A pipelined implementation," in *Proc. Int. Symp. Broadband Commun. (ISBC)*, 2010, pp. 11–14.
- [36] G. Sarkis, P. Giard, A. Vardy, C. Thibeault, and W. J. Gross, "Fast polar decoders: Algorithm and implementation," *IEEE J. Sel. Areas Commun.*, vol. 32, no. 5, pp. 946–957, 2014.
- [37] M. Hanif and M. Ardakani, "Fast successive-cancellation decoding of polar codes: Identification and decoding of new nodes," *IEEE Commun. Lett.*, vol. 21, no. 11, pp. 2360–2363, 2017.
- [38] M. Mondelli, S. A. Hashemi, J. Cioffi, and A. Goldsmith, "Simplified successive cancellation decoding of polar codes has sublinear latency," in *Proc. IEEE Int. Symp. Inf. Theory (ISIT)*, 2020, pp. 401–406.
- [39] E. Sharon, S. Litsyn, and J. Goldberger, "Efficient serial message-passing schedules for LDPC decoding," *IEEE Trans. Inf. Theory*, vol. 53, no. 11, pp. 4076–4091, 2007.
- [40] S.-Y. Chung, T. Richardson, and R. Urbanke, "Analysis of sum-product decoding of low-density parity-check codes using a Gaussian approximation," *IEEE Trans. Inf. Theory*, vol. 47, no. 2, pp. 657–670, 2001.
- [41] G. Elidan, I. McGraw, and D. Koller, "Residual belief propagation: Informed scheduling for asynchronous message passing," in *Proc. 22nd Conf. Uncertainty Artif. Intell. Cambridge, MA, USA: MIT*, 2006, pp. 165–173.
- [42] X. Liu, Y. Zhang, and R. Cui, "Variable-node-based dynamic scheduling strategy for belief-propagation decoding of LDPC codes," *IEEE Commun. Lett.*, vol. 19, no. 2, pp. 147–150, 2015.

- [43] B. Wang, Y. Zhu, and J. Kang, "Two effective scheduling schemes for layered belief propagation of 5G LDPC codes," *IEEE Commun. Lett.*, vol. 24, no. 8, pp. 1683–1686, 2020.